Supplementary Information (SI) for New Journal of Chemistry.
This journal is © The Royal Society of Chemistry and the Centre National de la Recherche Scientifique 2026

Supporting Information

Docosahexaenoic acid-copper (DHA-Cu) complex catalysis: UV- activated aerobic oxidation via experimental and computational approaches

Arunadevi Mani[a], Janani Mullaivendhan [a], Velmurugan Loganathan [a], Idhayadhulla Akbar [a].*

[a] Research Department of Chemistry, Nehru Memorial College (Affiliated to Bharathidasan University), Puthanampatti -621007, Tiruchirappalli District, Tamil Nadu, India.

Corresponding author E-mail: a.idhayadhulla@gmail.com

1. **The FT-IR spectra detailed explanation about absorption frequency and functional group presentation of the DHA-Cu complex**

Table 1. The FT-IR spectra detailed explanation about absorption frequency and functional group presentation of the DHA-Cu complex

Absorption frequency (cm^{-1})	**Functional group present**	**Explanation**	**References**
DHA (Docosahexaenoic acid)			
411.55, 449.38, and 502.59 cm^{-1}	lower-frequency fingerprint region	distinct skeletal deformation and out-of-plane bending modes	2
1041.81	C–O stretching	C–O (from –COOH) bond stretch.	3
1638.00	C=C stretching	From cis-double bonds in the unsaturated hydrocarbon chain.	4
3269.74	O–H stretching (H-bonded)	Broad O–H stretch from the carboxylic acid group**,** possibly hydrogen bonded.	5
DHA-Cu complex			
591.64	Cu–O stretching vibrations	Indicates interaction between Cu and oxygen atoms in DHA.	1
797.98	C=C bending	Suggests presence of cis-double bonds in the unsaturated chain of DHA.	4
864.37	CH_2 rocking	Supports the presence of aliphatic and unsaturated hydrocarbon chains in DHA.	6
1046.62	C–O stretching	C–O bond stretch.	7
1638.00	C=C stretching (alkene)	Typical of unsaturated fatty acids; could be shifted due to coordination with Cu.	4
3433.93	O–H stretching (broad)	Strongly hydrogen bonded OH, possibly affected by metal coordination or moisture.	8

2. Proposed Photocatalytic Mechanism for DHA–Cu complex

2.1. Proposed Photocatalytic Mechanism for DHA–Cu complex

The proposed mechanism involving reactive oxygen species is based on previously reported photocatalytic oxidation pathways of copper complexes and represents a plausible reaction pathway.

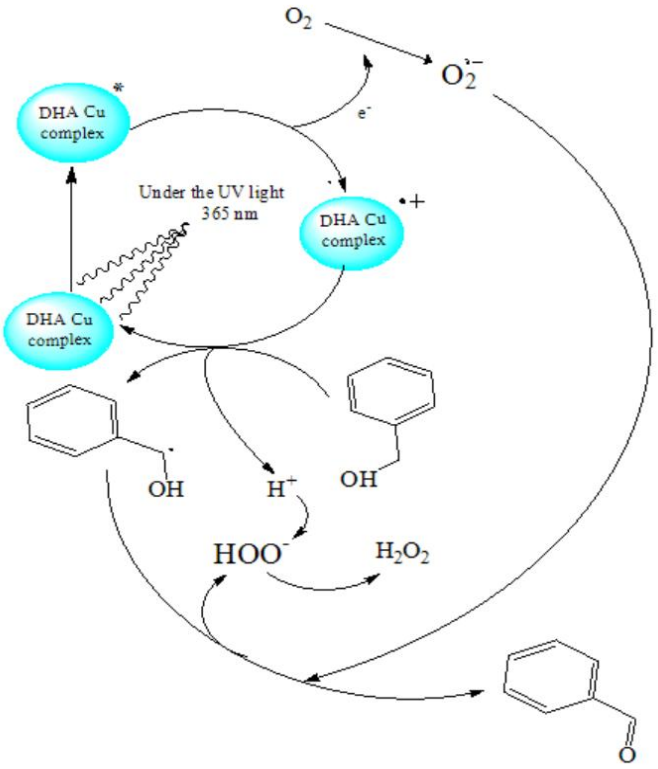

Scheme 1: Proposed possible Photocatalytic Mechanism for DHA–Cu complex

DHA-Cu complex under the UV-light irradiation, the DHA-Cu complex becomes excited and changes to an excited state. In this excited state, the DHA-Cu complex accepts an electron from benzyl alcohol and return to its normal ground state. Due to this electron transfer, benzyl alcohol forms a benzyl radical along with the release of H^+ ions. At the same time, the O_2 present in the reaction medium accepts an electron form ($^{\bullet}O_2^-$). These superoxide radicals react with H^+ ions to produce ($^{\bullet}OOH$). Further, the benzyl radical loses another hydrogen ion and gets converted into benzaldehyde and H_2O_2. The formation of these free radicals confirmed by EPR measurements using DMPO as a spin-trapping reagent and the conversion of benzyl alcohol to benzaldehyde was confirmed by GC analysis. Possible mechanism for photocatalytic oxidation of benzyl alcohol converted into benzaldehyde using the DHA-Cu complex under UV-light is shown in scheme 1.

3. The quantitative performance metrics such as turnover frequency (TOF), conversion yield, and selectivity, of the DHA-Cu complex

The conversion yield of benzyl alcohol and the selectivity of each product were determined from the gas chromatography (GC) results[10] (NMR Fig. 1. (a-b)) as follows:

3.1. Conversion of Benzyl Alcohol (%)

$$\text{Conversion (\%)} = \frac{\text{Initial peak area of benzyl alcohol} - \text{Remaining peak area}}{\textit{Initial peak area of benzyl alcohol}} \times 100$$

Initial peak area = Benzyl alcohol + Benzaldehyde = 21.64 + 28.97 = 50.61

Remaining benzyl alcohol = 21.64

$$\text{Conversion (\%)} = \frac{50.61 - 21.64}{50.61} \times 100$$

Conversion = 57.3%

3.2. Selectivity toward Benzaldehyde (%)

$$\text{Selectivity (\%)} = \frac{\text{Peak area of benzaldehyde}}{\text{Total product formed}} \times 100$$

Product formed = total benzyl alcohol converted = 50.61 − 21.64 = 28.97

Benzaldehyde = 28.97

$$\text{Selectivity (\%)} = \frac{28.97}{28.97} \times 100$$

Selectivity (%) = 100%

3.3. Turnover Frequency (TOF)

$$\text{TOF} = \frac{\text{Moles of product formed}}{\text{Moles of catalyst} \times \text{reaction time}}$$

$$\text{TOF} = \frac{0.0573}{0.01 \times 15\ (\text{min})}$$

TOF = 0.382 min^{-1}

The TOF seems lower because the conversion is only 57% after 15 min. The catalytic performance was evaluated using the oxidation of Benzyl alcohol as a model reaction. The reaction showed 80% conversion with 94% selectivity toward Benzaldehyde after 1 h of UV irradiation. The calculated TOF was 75 h^{-1}, demonstrating efficient catalytic activity. The catalyst also exhibited good recyclability over multiple reaction cycles.

4. The DHA-Cu complex ^{1}H, and ^{13}C NMR spectrum of benzaldehyde

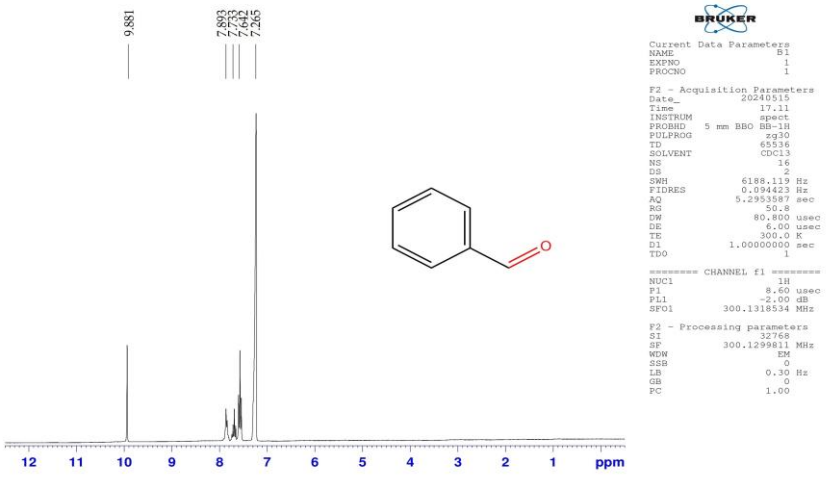

(a) ^{1}H NMR

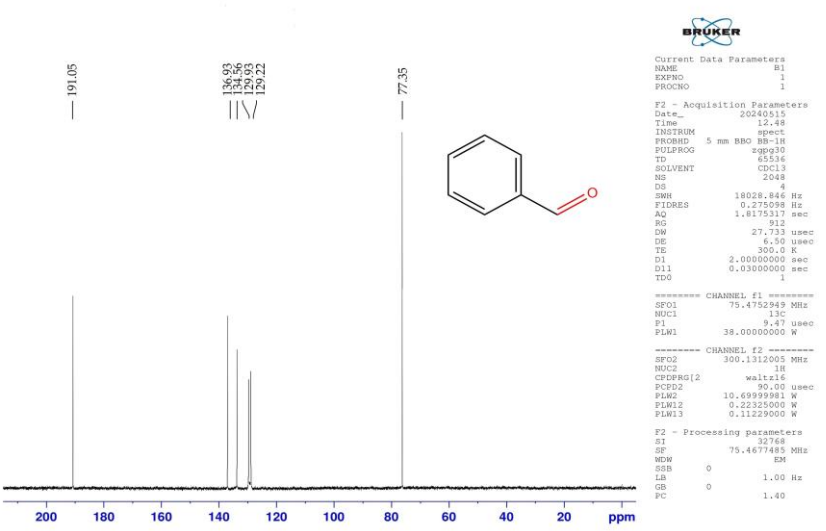

(b) ^{13}C NMR

Fig. 1. NMR spectrum by benzaldehyde

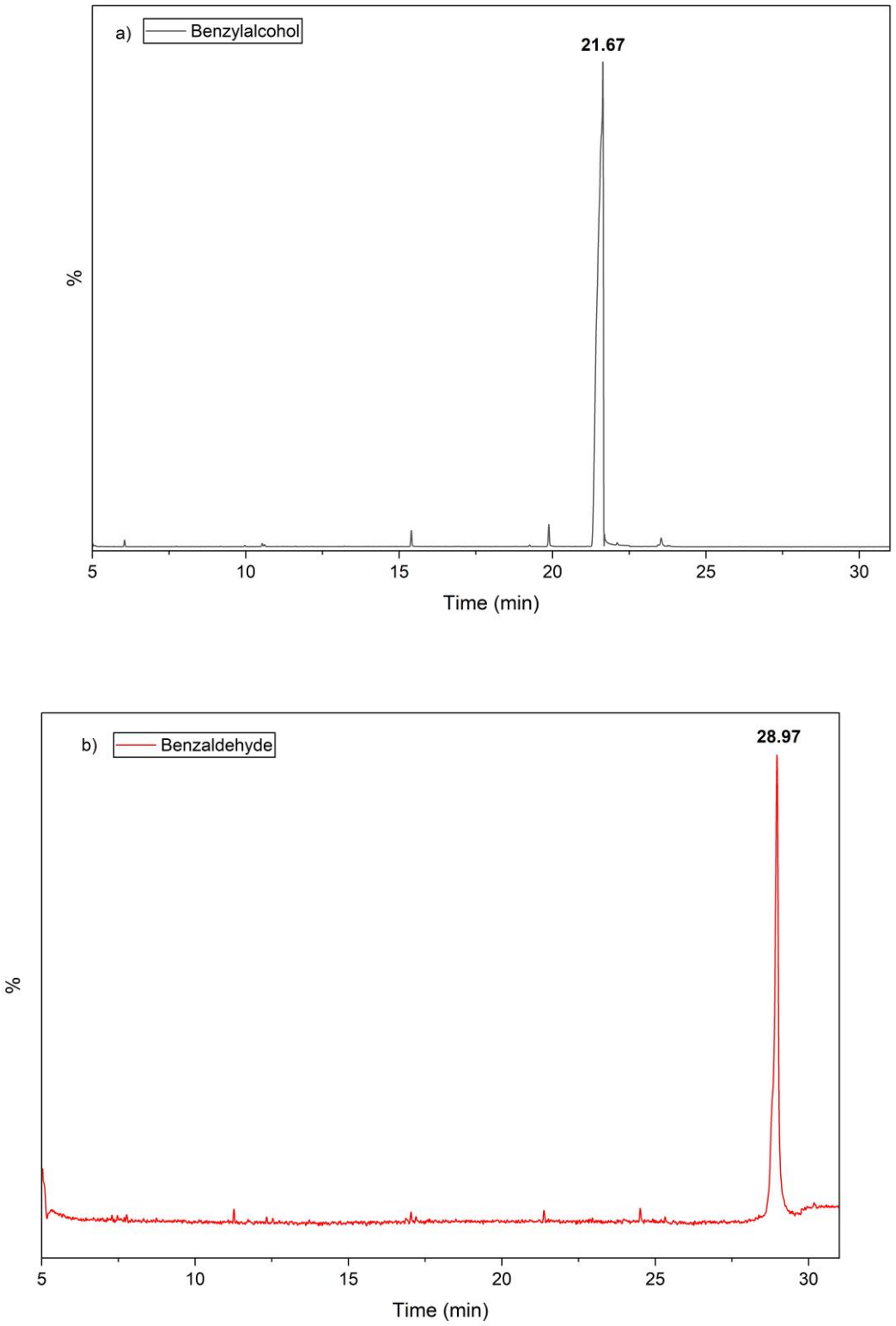

Fig. 2. GC chromatogram (a) before aerobic oxidation benzylalchol (b) after aerobic oxidation of benzaldehyde using DHA-Cu complex

5. The connection between IR and HOMO-LUMO value of the DHA–Cu complex

IR Peak	Possible Bond	Bond Reason	DFT Connection
591.64 cm^{-1}	Cu–O stretching (metal–ligand bond)	Formation of Cu–O bond changes the local electron density, reflecting in the low-frequency IR region.	Low HOMO (–0.21) means electrons are slightly bound, allowing Cu^{2+} to interact with lone pairs on oxygen. Soft molecule (s = 22.2) allows this bond to form easily, altering the IR spectrum.
797.98 cm^{-1}	Metal–ligand vibrations	Slight red/blue shift reflects metal coordination environment changes (Cu).	HOMO–LUMO gap (0.09 eV) allows fast charge redistribution upon metal interaction → shifts vibrational energy. Reflects soft-soft interaction: polarizable groups interacting with metal centers.
864.37 cm^{-1}	Out-of-plane bending M–O interaction	Minimal shift due to stable C–H framework but affected by nearby Cu.	Ionization energy (0.21 eV) means moderate ability to lose electrons → Cu can alter π-clouds slightly. Local dipole change shows up in IR bending modes.
1041.81 cm^{-1}	C–O stretching	Coordination with carbon–oxygen bond electron density.	Chemical potential (μ = –0.17) indicates electron flow from DHA to metal centers. Softness allows electron sharing → altered bond stiffness shifted to the IR peak.

1384.50 cm^{-1}	Symmetric stretching – CH_3	Metal coordination changes the vibration energy of CH_3 groups.	Electron affinity (0.12) of the system shows the molecule easily accepts small charge perturbations. CuO possibly increases electron withdrawal → blue shift observed (1384 → 1397).
1621.35 cm^{-1}	C=C stretching (conjugated system)	These are core π-system vibrations and are sensitive to conjugation changes.	ΔE = 0.09 eV indicates high π-electron mobility → C=C, Cu interaction. Electrophilicity (0.32) favors π-back bonding or delocalization, stabilizing structure.
3435.93 cm^{-1}	O–H stretching (hydroxyl groups in DHA)	Extending and slight shift due to hydrogen bonding and metal interaction.	Soft molecule + polar groups = flexible hydrogen bonding Electronegativity (χ = –0.17) suggests electron-donating groups are available for bonding, changing OH stretch.

6. Reference

1. A. S. Pujar, A. B. Kulkarni, S. N. Mathad, C. S. Hiremath, M. K. Rendale, M. R. Patil, R. B. Pujar, *Int. J. Self-Propag. High-Temp. Synth.*, 2018, **27**, 174-179.

2. B. Behera, K. Takahashi, Y. P. Lee, *PPCP.*, 2022, **24**, 18568-18581.
3. O. A. B. Pires, R. T. Alarcon, C. Gaglieri, L. C. da Silva-Filho, G. Bannach, *J. Therm. Anal. Cal.*, 2019, **137**, 171-173.
4. T. Rihayat, A. E. Hadi, N. Aidy, A. Safitri, J. P. Siregar, T. Cionita, D. F. Fitriyana, *Polym.*, 2021, **13**, 4019.
5. S. Kumari, Sunaina, S. Devi, M. Jha, *Energ & Fuels.*, 2025, **39**, 6426-6437.
6. A. E. Lewandowska, N. H. Inai, O. R. Ghita, S. J. Eichhorn, *RSC adv., 2018*, **8**, 35831-35839.
7. P. T. Shoko, E. W. Blanch, P. J. Torley, C. Pillidge, *J. Raman Spectrosc.*, 2024, **55**, 1146-1155.
8. W. S. Kang, S. W. Choi, H. S. Kim, J. H. Kim, J. H. Lee, *J. anal. sci. Technol.*, 2024, **15**, 34.